Clinical Cancer Research

Combining Vascular Normalization with an Oncolytic Virus Enhances Immunotherapy in a Preclinical Model of Advanced-Stage Ovarian Cancer

Kathy Matuszewska[1], Lisa A. Santry[2], Jacob P. van Vloten[2], Amanda W.K. AuYeung[2], Pierre P. Major[3], Jack Lawler[4], Sarah K. Wootton[2], Byram W. Bridle[2], and Jim Petrik[1]

Abstract

Purpose: Intravenous delivery of oncolytic viruses often leads to tumor vascular shutdown, resulting in decreased tumor perfusion and elevated tumor hypoxia. We hypothesized that using 3TSR to normalize tumor vasculature prior to administration of an oncolytic Newcastle disease virus (NDV) would enhance virus delivery and trafficking of immunologic cell subsets to the tumor core, resulting in systemically enhanced immunotherapy and regression of advanced-stage epithelial ovarian cancer (EOC).

Experimental Design: Using an orthotopic, syngeneic mouse model of advanced-stage EOC, we pretreated mice with 3TSR (4 mg/kg per day) alone or followed by combination with fusogenic NDV(F3aa) (1.0×10^8 plaque-forming units).

Results: Treatment with 3TSR normalized tumor vasculature, enhanced blood perfusion of primary EOC tumors, and induced disease regression. Animals treated with combination therapy had the greatest reduction in primary tumor mass, ascites accumulation, and secondary lesions (50% of mice were completely devoid of peritoneal metastases). Combining 3TSR + NDV(F3aa) led to enhanced trafficking of immunologic cells into the primary tumor core.

Conclusions: We have shown, for the first time, that NDV, like other oncolytic viruses, is a potent mediator of acute vascular shutdown and that preventing this through vascular normalization can promote regression in a preclinical model of advanced-stage ovarian cancer. This challenges the current focus on induction of intravascular thrombosis as a requisite for successful oncolytic virotherapy.

See related commentary by Bykov and Zamarin, p. 1446

Introduction

Ovarian cancer is the leading cause of death among all malignancies affecting the female reproductive tract (1). Known as "The Whispering Disease," ovarian cancer presents with vague symptoms, such as abdominal pain, swelling, and indigestion, and lacks effective screening techniques (2). This lack of specific symptomology typically results in diagnosis at late stages, when the 5-year survival rate is as low as 26%, and clinical treatment strategies have reduced efficacy (1). The standard of care for late-stage disease has remained unchanged for decades and involves surgical cytoreduction followed by platinum- and taxane-based chemotherapy (3). The high propensity of chemoresistance to these agents reflects the need for innovative therapies to reduce the high mortality associated with this silent killer (4).

The idea of whether an immune response can be produced against neoplastic cells to eliminate cancer has long been contemplated (5). The role of the immune system in tumorigenesis was initially suggested based on observations of a greater incidence of cancer in immunodeficient mice and the unveiling of tumor-associated antigens (TAA; ref. 6). In recent years, immunotherapy—a group of treatments aimed at enhancing the body's immune system to fight cancer—has emerged as a new pillar of cancer treatment (7). A number of agents, such as PD-1–specific monoclonal antibodies to block inhibitory pathways downstream of antigen recognition (Keytruda, Merck) or personalized therapeutic vaccines aimed at reprogramming the immune system against cancer (Sipuleucel-T, Dendreon), have acquired FDA approval in the treatment of lung and prostate cancers, respectively (8, 9). Although no FDA-approved immunotherapy for ovarian cancer exists, research correlating increased progression-free survival with greater influx of T cells in tumors of patients with advanced ovarian carcinoma, and the emergence of epithelial ovarian cancer (EOC)–associated antigens, reflect the candidacy of EOC for immune-based treatments (10, 11).

The recent approval of a modified herpes virus (T-Vec, Amgen) as a drug for the treatment of melanoma has increased interest in

[1]Department of Biomedical Sciences, University of Guelph, Guelph, Ontario, Canada. [2]Department of Pathobiology, University of Guelph, Guelph, Ontario, Canada. [3]Department of Oncology, McMaster University, Hamilton, Ontario, Canada. [4]Department of Pathology, Beth Israel Deaconess Medical Center, Boston, Massachusetts.

Note: Supplementary data for this article are available at Clinical Cancer Research Online (http://clincancerres.aacrjournals.org/).

K. Matuszewska and L.A. Santry contributed equally to this article.

J.P. van Vloten and A.W.K. Au Yeung contributed equally to this article.

S.K. Wootton and B.W. Bridle contributed equally to this article.

Corresponding Author: Jim Petrik, University of Guelph, Guelph, ON N1G 2W1, Canada. Phone: 519-824-4120, ext. 54921; E-mail: jpetrik@uoguelph.ca

doi: 10.1158/1078-0432.CCR-18-0220

Translational Relevance

Ovarian cancer is a disease for which treatment efficacy has not changed appreciably in decades. This article describes a therapeutic approach that could dramatically improve our ability to treat women with advanced-stage ovarian cancer. We have shown that treatment with the TSP-1 peptide 3TSR induces tumor regression and promotes vascular normalization. The resultant improvement in tumor tissue perfusion and reduced tumor hypoxia decreased the immunosuppressive tumor environment and increased oncolytic viral-induced uptake of immune cells. 3TSR inhibited the vascular shutdown induced by Newcastle disease virus (NDV) and combination therapy with 3TSR and NDV(F3aa) reduced primary tumor growth and metastatic disease compared with controls and each treatment as a monotherapy. We anticipate rapid translation of this approach into a clinical trial in women with advanced-stage ovarian cancer. NDV has a rich history of efficacy in gynecologic malignancies and, combined with 3TSR, offers the opportunity to dramatically improve survival from this disease.

the field of oncolytic virotherapy and the potential immunostimulatory roles of these agents (12). Oncolytic viruses (OV) preferentially infect and kill tumor cells while leaving normal somatic cells intact (12). In the process, these agents also instigate innate immunologic cell trafficking in response to viral and cell death–associated proteins, resulting in enhanced cross-priming of adaptive immune cells against TAAs (13). Newcastle disease virus (NDV) is an avian paramyxovirus with longstanding benefit as an oncolytic agent in animal models (14). NDV has the longest history of clinical trial testing of any OV and has demonstrated efficacy against a variety of cancers including advanced colorectal (15), breast (16), ovarian (17), and metastatic renal cell (18) cancers, with partial or complete responses reported in each. NDV has been shown to overcome the immunosuppressive tumor microenvironment and can directly lead to the induction of immune responses due to increased production of cytokines, especially interferon (IFN; ref. 13). Cleavability of the fusion protein of NDV is a major determinant of its virulence, lending potential for the modification of this protein to enhance therapeutic efficacy (19).

Although a number of studies have demonstrated the effectiveness of intratumoral delivery of OVs to treat primary tumors, the location of some tumors and/or dissemination of metastases makes it an impractical route of delivery (20). OVs can be delivered systemically, which allows for virus-mediated lysis of microscopic secondary tumors that cannot be resected during cytoreductive surgery. However, a consequence of systemic OV therapy is the initiation of vascular shutdown within the tumor following uptake (21–23). Initially, this vascular shutdown was viewed as a potential benefit of OV therapy, by sequestering virus and therefore maximizing direct oncolysis (22, 24). However, the maximum impact of OVs is now thought to result from their use as cancer vaccines using repeat dosages to induce greater intratumoral immunity (25). If OVs induce vascular disruption, uptake of subsequent doses of OV, or trafficking of immune cells to the tumor will be significantly impaired. Our approach to normalizing the tumor vasculature and preventing the OV-induced vascular shutdown represents a paradigm shift in OV tumor therapy.

In order to meet oxygen and nutrient demands, tumors initiate a crude version of the process of angiogenesis by secreting factors such as vascular endothelial growth factor (VEGF) in response to hypoxia, oncogenes, and loss-of-tumor suppressor genes (26). The resultant vessels are plagued by structural abnormalities such as irregular branching, loss of basement membrane integrity, and inadequate or absent perivascular cells, cumulating in heterologous flow and increased vessel permeability (27). The inefficiency of these vessels hinders delivery of cancer therapies, such as chemotherapy, to the tumor core (28). This limited vascular perfusion also selects for hypoxia and acidity in the tumor microenvironment, which have been shown to limit drug effectiveness and exacerbate metastasis (29). The current therapeutic strategy of "vascular normalization" uses molecules that inhibit proangiogenic factors or upregulate antiangiogenic factors to restore a proper balance of these signals and repair tumor vasculature (30). Blocking VEGF is the most common method to achieve vascular normalization, and anti-VEGF agents such as bevacizumab have had clinical success against cancer, primarily when combined with chemotherapy (31). However, anti-VEGF therapies have been associated with side effects such as gastrointestinal perforation and venous thromboembolism (32).

Thrombospondin-1 is a naturally occurring inhibitor of angiogenesis found on the cell surface and extracellular matrix of various cell types (33). This protein contains three homologous thrombospondin type 1 repeat domains (3TSR) that harbor the majority of its antiangiogenic properties through association of the CD36 receptor on endothelial cells, leading to inhibition of endothelial cell proliferation and migration (34, 35). As an antiovarian cancer agent, 3TSR also has the added benefit of directly inhibiting tumor cell proliferation and migration through TGFβ activation (36). As a small bioactive recombinant peptide, 3TSR has been shown to have significant antitumor effects in various models either alone or in combination with chemotherapy (35, 37). 3TSR potently induces vascular normalization in a murine model of advanced-stage EOC and enhances tumoral uptake of chemotherapy drugs delivered intraperitoneally (37).

We hypothesized that pretreatment with 3TSR ahead of NDV delivery would abate the vascular shutdown common with oncolytic virus therapy and increase the quantity of viruses and immunologic cells that infiltrate the tumor, leading to regression of advanced-stage EOC.

Materials and Methods

Reagents and cell lines

Spontaneously transformed murine ovarian surface epithelial cells (ID8; generously donated by Drs. K. Roby and P. Terranova, Kansas State University, Manhattan, KS) and human progressive ovarian epithelial adenocarcinoma cells (CAOV-3; ATCC) were cultured in Dulbecco's modified Eagle medium (DMEM, Gibco) with 10% FBS and 1% antibiotic/antimycotic (ABAM; Gibco). Normal human ovarian surface epithelial (NOSE) cells (generously donated by Dr. J. Liu, MD Anderson Cancer Center, Houston, TX) were cultured in DMEM (Gibco) with 10% FBS, 1% antibiotic/antimycotic (ABAM; Gibco) and 2% L-glutamine. 3TSR was generated with recombinant versions of the 3 Type I repeats of Thrombospondin-1 as previously described (37).

Mouse model

All mice were purchased from the Charles River Laboratories and housed in accordance with the Canadian Council on Animal Care and approved by the Animal Care Committee at the University of Guelph. Tumors were induced as described previously (38), in generation of an orthotopic, syngeneic, immunocompetent mouse model of EOC. Briefly, ID8 cells (1.0×10^6 in 6 μL) were injected directly under the left ovarian bursa of C57Bl-6 mice using a Hamilton syringe (Fisher Scientific). At 60 days after tumor induction (PTI), mice form large ovarian masses, numerous secondary peritoneal lesions, and accumulate abdominal ascites, which replicates the symptoms of women with stage III (advanced) EOC. Mice ($n = 12$–15 per group) were left untreated or treated with either 3TSR (4 mg/kg, intraperitoneal injection, once daily starting at day 60), NDV(F3aa; 1.0×10^8 PFU, intravenous injection, one time on day 74), or a combination of both. Mice were euthanized 90 days after tumor induction. Immediately, primary tumors were collected, and the peritoneum was assessed for metastatic spread using a lesion scoring system that was previously reported (38). Briefly, abdomens with no visible secondary tumors were scored a 0, presence of one or two secondary lesions scored a 1, three to 10 lesions were scored 2, and >10 lesions received a score of 3.

Production of NDV

NDV(F3aa) carrying a transgene encoding full-length enhanced green fluorescent protein (GFP) was rescued using plasmids kindly provided by Dr. Peter Palese (Mount Sinai School of Medicine, New York, NY) and a recombinant modified vaccinia virus (Ankara strain) expressing T7 RNA polymerase and amplified in specific pathogen-free embryonated chicken eggs as previously reported (39). NDV(F3aa)-GFP-containing allantoic fluid was harvested and clarified by centrifugation ($1{,}500 \times g$). The virus was first filtered using Supracap TM 50 Depth Filter Capsules (Pall), followed by purification and concentration by tangential flow filtration using a Centramate LV holder (Pall) and a 100 kDa Omega Screen channel-cassette. Next, NDV underwent a sucrose gradient centrifugation using a SW41 rotor at $120{,}000 \times g$ for 3.5 hours to remove contaminating chicken host proteins, where the virus was collected between the 40% and 50% sucrose band. Finally, viruses were dialyzed in PBS using a 10-kDa Slide-A-Lyzer dialysis cassette (Thermo Fisher Scientific) to remove any remaining sucrose. Purified viruses were aliquoted and directly frozen (−80°C) until use. Viruses were titrated using DF-1 cells by the 50% tissue culture infective dose ($TCID_{50}$) method and calculated using the Spearman–Karber method (40). For each treatment, virus aliquots were taken from the −80°C freezer, thawed on ice, and diluted to the appropriate volume with PBS.

Cell viability assays

ID8, CAOV-3, and NOSE cells were seeded in 96-well plates (1×10^4 cells/well). The next day, cells were infected in triplicate with the indicated viruses at various multiplicities of infection (MOI; 0.2–50 PFU/cell). Following a 48-hour incubation, resazurin (resazurin sodium salt; Millipore-Sigma) was added to a final concentration of 20 μg/mL. After a 4-hour incubation, the fluorescence was read at excitation and emission wavelengths of 535/25 nm and 590/35 nm, respectively. These assays were repeated in triplicate.

Cell growth curve

ID8 (2.5×10^4 cells/well), CAOV-3 (2.5×10^4 cells/well), and NOSE (5×10^4 cells/well) cells were seeded into 12-well plates. The next day, cells were infected in triplicate with an MOI of 0.5 or mock infected (1× PBS). Cells were harvested at 24, 48, and 72 hours after infection (p.i.) and counted. Dead cells were excluded by trypan blue staining.

Apoptosis assay

ID8 (2.5×10^4 cells/well), CAOV-3 (2.5×10^4 cells/well), and NOSE (5×10^4 cells/well) cells were seeded into 12-well plates. The next day, cells were infected in triplicate with an MOI of 0.1 or mock infected (1× PBS). Cells were harvested at 24 hours p.i. and stained for Annexin V (Thermo Fisher Scientific) and 7-aminoactinomycin D (7AAD; Thermo Fisher Scientific) and analyzed by fluorescence-activated cell sorting (FACS).

One-step viral growth curves

Cells were infected with NDV(F3aa)-GFP at an MOI of 0.5 in basal DMEM for 1 hour, rocking at room temperature. Cells were then washed 2× with PBS and incubated at 37°C. Aliquots (500 μL) were taken in triplicate at 8, 12, 24, and 48 hours p.i., and titers were assessed by $TCID_{50}$ in DF-1 cells.

IFN-sensitivity assay

ID8 cells were seeded in 96-well plates (1×10^4 cells/well). Cells were pretreated with or without an anti-IFNAR antibody (Bio X Cell) at a concentration of 10 μg/mL. An hour later, cells were pretreated with increasing amounts of recombinant murine IFNβ (eBioscience) ranging from 0 to 6,000 pg/mL for 2 hours coupled with or without infection with NDV(F3aa)-GFP (MOI = 12.5). Viability was assessed after 72 hours using the previously described resazurin assay. The percentage of live cells was determined by normalization to mock-infected controls. This assay was repeated in triplicate.

IFNβ ELISA

ID8 (2.5×10^4 cells/well), CAOV-3 (2.5×10^4 cells/well), and NOSE (5×10^4 cells/well) cells were seeded in a 12-well plate and left to adhere overnight. The next day, cells were infected in triplicate at an MOI of 0.5, and supernatant was collected at 12, 24, 48, and 72 hours p.i. A mock-infected control was included, and supernatant was collected at 72 hours. LumiKine Xpress mIFNβ and hIFNβ kits (InvivoGen) were used according to the manufacturer's protocols, and quantities of mIFNβ and hIFNβ were calculated using a standard curve.

IHC

Primary ovarian tumors collected 90 days PTI were fixed in 10% neutral buffered formalin overnight, washed with 70% ethanol for 24 hours, and transferred to PBS. Tissues were embedded in paraffin wax and cut into 5-μm sections using a rotary microtome. Prior to staining, tissues were deparaffinized using reagent-grade xylene and subjected to a series of decreasing ethanol concentrations for rehydration. Endogenous peroxidase activity was quenched through a 10-minute incubation period in 3% hydrogen peroxide followed by antigen retrieval using citrate buffer with Tween 20. To reduce nonspecific binding of antibodies, samples were blocked in 5% bovine serum albumin (with 0.02% sodium azide) for 10 minutes at room temperature. Tumor sections were exposed to the following primary antibodies

overnight at 4°C to assess infiltration of immunologic cell subpopulations: anti-CD68 (1:100, Novus), anti-CD8 (1:200, Novus), anti-CD4 (1:1,000, Abcam), anti-NKG2D (1:200, Abcam), anti-Foxp3 (1:1,000, Abcam), anti-CD138 (1:400, Stemcell), and antineutrophil (1:200, Abcam). Biotin-conjugated secondary antibodies (1:100; Invitrogen) were added for 2 hours at room temperature, followed by treatment with ExtrAvidin (1:50, Sigma-Aldrich) for 1 hour. Tissues were exposed to SigmaFast 3,3′-diaminobenzidine (DAB; Sigma-Aldrich) for visualization of staining and counterstained using Carazzi's hematoxylin. For each slide, areas of greatest positive staining within the tumor core were captured ($n = 8$ tumors per experimental group, 3–4 areas of interest per section). Histologic analysis was performed by manual count of cell nuclei and reported as a percentage against total cell nuclei.

Immunofluorescence: Vascular normalization

Tumors from each of the 4 treatment groups [PBS, 3TSR only, NDV(F3aa) only, and 3TSR + NDV(F3aa)] were collected at day 90, embedded in cryomatrix, and flash frozen. Cryosections (5 μm) were mounted on slides. Sections were fixed using reagent-grade acetone and stored at −20°C. Frozen sections were washed with PBS, and nonspecific binding was blocked using 5% bovine serum albumin in PBS for 10 minutes. Sections ($n = 4$ tumors per experimental group, 3–4 areas of interest per section) were subjected to immunofluorescence colocalization, in which they were simultaneously stained overnight using anti-CD31 (1:50, Abcam) to detect vascular endothelial cells and anti-alpha-smooth muscle actin (α-SMA; 1:600, Sigma) to identify vascular pericytes. Slides were stained with secondary antibodies against anti-CD31 (Alexa Fluor594nm, red, 1:100) and α-SMA (Alexa Fluor488nm, green, 1:100) for 1 hour at room temperature. Slides were counterstained and cured using Prolong Gold anti-fade mountant with DAPI. Representative images (3–4 per section, 200× magnification) were obtained under both the 594-nm and 488-nm channels using an inverted fluorescent microscope (Olympus) and Metamorph imaging software (Burlingame). These images were overlaid using Metamorph, and normalized vasculature was reported as the percentage of blood vessels exhibiting CD31 and α-SMA double-positive staining in each treatment group.

Immunofluorescence: Tissue hypoxia

Primary tumors from each treatment group were collected during necropsy at 90 days PTI and processed as described for IHC. Sequential tumor sections were mounted on slides (2 sections per slide) and deparaffinized as described. Endogenous peroxidase activity and nonspecific binding were blocked using 0.02% sodium borohydride in PBS for 12 minutes and 5% bovine serum albumin for 15 minutes, respectively. Sections were subjected to immunofluorescence colocalization, in which they were stained with anti-CD31 (1:25) and anti-α-SMA (1:600) simultaneously, at 4°C overnight. Sections were stained with secondary antibodies against anti-CD31 (Alexa Fluor594nm, red, 1:100) and α-SMA (Alexa Fluor488nm, green, 1:100) for 1 hour at room temperature. Tissues were once again blocked with 5% bovine serum albumin for 5 minutes and exposed to antihypoxyprobe-1 antibody (1:25, Hypoxyprobe) at 4°C overnight. Sections were stained with a secondary antibody against hypoxyprobe-1 (Alexa Fluor594nm, red, 1:150) for 1 hour at room temperature. Slides were counterstained and cured using Prolong Gold antifade mounting medium. Representative images ($N = 4$ tumors per experimental group, 3–4 areas of interest per section, 200× magnification) were obtained for both the CD31/ α-SMA colocalized sections and hypoxyprobe-1–stained sections. Sequential sections were overlaid, and hypoxia was pseudocolored blue using Metamorph software.

Western blot analysis: Expression of immunosuppressive cytokines

Tumor tissues were collected at 90 days PTI from mice treated with PBS control ($n = 3$) or 3TSR (4 mg/kg/day IP starting at 60 days PTI; $n = 3$) and were prepared in RIPA lysis buffer containing protease and phosphatase inhibitors and protein concentrations were determined using a DC protein assay (Bio-Rad Laboratories). Samples (40 μg of total protein) were boiled in a denaturing SDS sample buffer and subjected to SDS-PAGE using either 8% or 15% resolving gels. Proteins were transferred to polyvinylidene difluoride PVDF membranes (Bio-Rad Laboratories) and blocked at room temperature for 1 hour in 5% skim milk with TBST. Membranes were probed overnight at 4°C for anti-VEGF (1:600 Abcam), anti-CCL22 (1:600; Abcam), anti-IL6 (1:1,000; Cell Signaling Technology), anti-IL-10 (1:500; Abcam), or anti-TGFβ1 (1:800; Abcam). Following washes with TBST, membranes were incubated for 1 hour at RT with appropriate IgG HRP-linked secondary antibodies (Cell Signaling Technology, Inc.). Antibody expression was visualized with Western Lightning Chemiluminescence Reagent Plus (PerkinElmer BioSignal, Inc.). To ensure equal loading of samples, blots were probed with GAPDH (1:1,000; Cell Signaling Technology) for 1 hour at room temperature followed by anti-rabbit IgG secondary antibody for 1 hour at room temperature. Computer-assisted densitometry was performed using AlphaEase FC software (AlphaInnotech), and results were quantified and reported as integrated densitometry values relative to GAPDH.

Statistical analysis

GraphPad Prism v7 software (Prism v7; GraphPad Software, Inc.) was used for statistical analysis and graph preparation. Each *in vitro* treatment group was represented by at least 3 biological replicates (repeated in triplicate) in all experiments. Data from the *in vitro* model were analyzed using a one-way ANOVA, and a Tukey test was used to determine statistical differences among treatment group means. A two-way ANOVA was performed for *in vivo* data and was also followed by a Tukey *post hoc* test. Differences among treatment groups were considered significant if $P < 0.05$. Graphs are presented as means per group ± SEM.

Results

Combination antiangiogenic (3TSR) and oncolytic virus [NDV(F3aa)] therapy induces regression of advanced-stage ovarian cancer *in vivo*

In our orthotopic, syngeneic mouse model of EOC, we started treatment with 3TSR at 60 days PTI to replicate the stage of disease progression in which the majority of women are diagnosed. Compared with saline controls, mice treated with 3TSR or NDV(F3aa) alone had significantly ($P < 0.01$) reduced primary tumor size at endpoint (90 days PTI). Mice undergoing combination therapy yielded the greatest reduction in primary disease at endpoint compared with saline controls ($P < 0.0001$) as well as either treatment alone (Fig. 1A). Consistent with our hypothesis that vascular normalization using 3TSR would abate

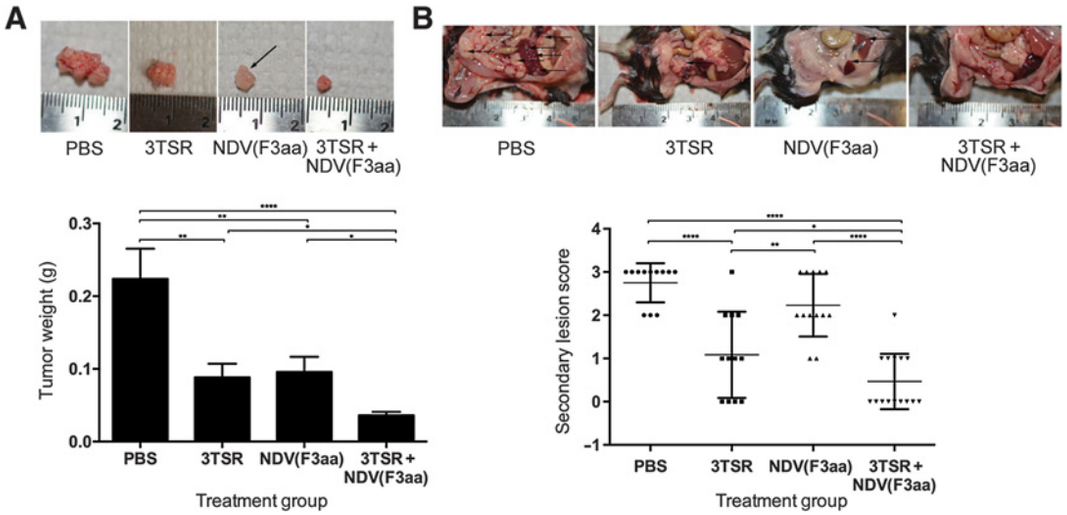

Figure 1.

Combined vascular normalization and oncolytic virus therapy induce significant regression of advanced-stage ovarian cancer. Mice were injected with 1×10^6 ID8 cells under the ovarian bursa, and tumors were allowed to develop without intervention until 60 days PTI. At this stage, mice exhibited disease similar to that of women with stage III ovarian cancer, and either received 4 mg/kg 3TSR i.p. for 15 days, a one-time i.v. injection of 1.0×10^8 PFU NDV(F3aa) at day 74 PTI, or a combination of both. At day 90 PTI, mice were sacrificed, and primary tumors were collected and weighed. **A,** All treatments significantly ($P < 0.01$) decreased primary tumor weight at endpoint, compared with PBS-treated controls. Combination 3TSR + NDV(F3aa) treatment yielded the largest reduction in primary tumor weight. All animals treated with NDV(F3aa) alone exhibited blanched tumors (arrows) consistent with vascular shutdown. **B,** All treatment groups had significantly reduced ($P < 0.05$) numbers of secondary lesions at endpoint compared with controls. Fifty percent of the animals in the 3TSR + NDV(F3aa) combination group were completely devoid of secondary tumors at endpoint. Metastatic lesions are indicated with arrows. Means ± SEM are shown. Data represent results from three separate animal trials ($N = 12$–15 per experimental group). Data were analyzed by one-way analysis of variance with the Tukey multiple comparison test; *, $P < 0.05$; **, $P < 0.01$; ****, $P < 0.0001$.

the vascular shutdown caused by an oncolytic virus, primary tumors retrieved from NDV(F3aa)-only–treated mice were highly blanched and appeared to have reduced vascular perfusion (Fig. 1, arrow), whereas this was not observed in mice treated with 3TSR.

The effect of 3TSR and NDV(F3aa) on the extent of secondary lesions was also evaluated. At necropsy, the peritoneal cavities of mice were examined for visible secondary lesions, and each mouse was scored according to a grading system previously described (39). All treatments resulted in a significant decrease in the number of secondary lesions compared with sham-treated controls ($P < 0.01$). Animals treated with combination therapy had less secondary lesions than all other groups tested, and 50% of animals in the 3TSR + NDV(F3aa) group were completely devoid of visible secondary lesions at endpoint (Fig. 1B). Ascites fluid was collected, and the volume of fluid was measured for each mouse. There was a significant reduction in ascites volume in animals treated with both 3TSR and NDV(F3aa) compared with controls (Supplementary Fig. S1).

3TSR induces a potent vascular normalization, which is associated with significantly reduced tumor tissue hypoxia

We characterized the vascular density and maturity in tumors collected from the various treatment groups. CD31 and α-SMA were evaluated in cryosections of primary tumors at 90 days PTI by immunofluorescence microscopy to quantify the extent of tumor vascularization and the proportion of mature vessels. Quantification of the total number of CD31- and α-SMA–positive blood vessels per field of view revealed a significantly greater proportion of pericyte-covered vessels in groups treated with 3TSR ($P <$ 0.0001). NDV(F3aa)-only–treated animals presented with primary tumor vessels that had phenotypic loss of structure and focal necrosis. Combining NDV(F3aa) with 3TSR yielded luminal, pericyte-covered vessels more characteristic of those found in normal capillary beds (Fig. 2A).

We evaluated tumor tissue perfusion with and without 3TSR-induced vascular normalization. At 90 days PTI, mice were injected with 60 mg/kg weight hypoxyprobe-1 i.p. 2 hours prior to endpoint. Hypoxyprobe-1 distributes to all tissues, causing formation of thiol adducts in cells with an oxygen concentration of less than 14 μmol/L (41, 42). IHC was then performed on primary tumor sections to probe for these hypoxic adducts as an indirect measure of vascular blood perfusion. Quantification of staining intensity per field of view revealed significantly ($P < 0.01$) decreased hypoxia, resulting from enhanced vascular perfusion in primary tumors of all mice treated with 3TSR compared with PBS or NDV(F3aa) alone (Fig. 2B). Further, we performed immunofluorescence colocalization imaging of vascular endothelial cells and vascular pericytes, followed by immunofluorescence imaging of hypoxyprobe-1 on sequential tumor sections to localize tumor hypoxia in the context of vascular maturity. Indeed, vessels within fields of view of low hypoxia had a significantly ($P < 0.01$) greater proportion of CD31- and α-SMA–positive vessels compared with highly hypoxic tissues (Fig. 2C). In order to further validate that normalized vasculature reduces hypoxia in tumors and increases oxygen diffusion distance, the average distance between vessels and the edge of hypoxic regions was measured. The average distance between normalized vessels and hypoxic regions was 113.76 μm, whereas this value for nonnormalized (αSMA-negative vessels) was 19.10 μm (Fig. 2D).

NDV(F3aa) significantly reduces the viability of ovarian cancer cells *in vitro*, while leaving normal cells intact

The direct oncolytic effects of NDV(F3aa)-GFP, assessed by a decrease in cell viability, were investigated in spontaneously transformed murine ovarian cancer cells (ID8) and human ovarian adenocarcinoma cells (CAOV-3). Cells were treated with NDV(F3aa)-GFP at increasing MOIs from 0 to 50 PFU/cell, and cytotoxicity was quantified using a resazurin cell

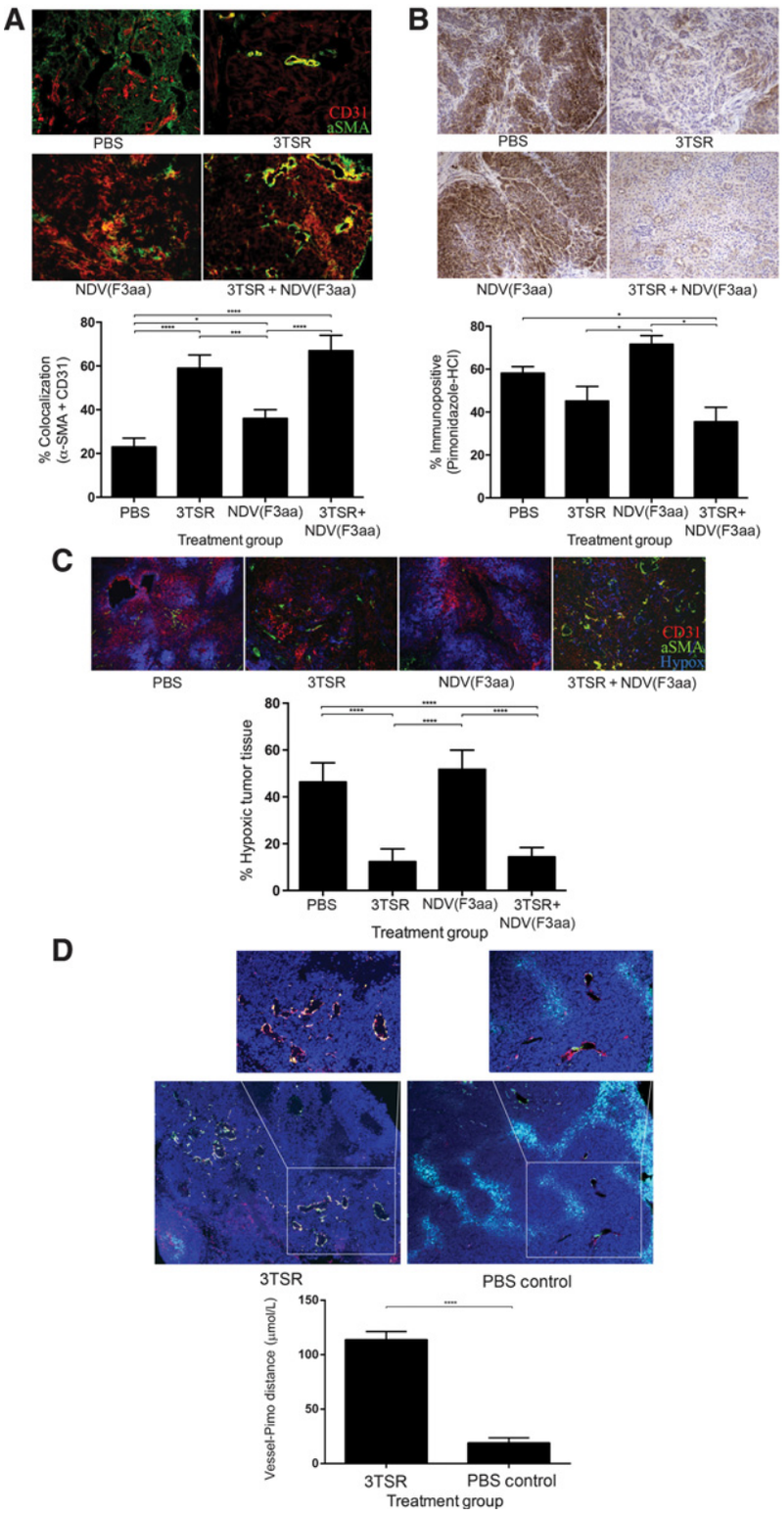

Figure 2.

3TSR pretreatment induces vascular normalization and reduces ovarian tumor hypoxia. Primary murine ovarian tumors were collected at day 90 PTI. **A,** Immunofluorescence colocalization of vascular endothelial cells (CD31, red) and vascular pericytes (α-SMA, green) was performed on frozen primary ovarian tumor sections from each of the treatment groups [PBS, 3TSR only, NDV(F3aa) only, and 3TSR + NDV(F3aa)]. Colocalization revealed an increased proportion of mature, pericyte-covered blood vessels in tumors of animals pretreated with 3TSR and phenotypic loss of vessel structure as well as focal necrosis in those treated with NDV(F3aa) alone. **B,** Pretreatment with 3TSR prior to delivery of NDV(F3aa) significantly ($P < 0.01$) decreased the formation of hypoxia-driven adduct formation in primary tumor tissues compared with NDV(F3aa) alone. **C,** Immunofluorescence trilocalization of vascular endothelial cells (CD31, red), vascular pericytes (α-SMA, green), and hypoxia (hypoxyprobe, blue) revealed that areas of EOC tumors surrounding abnormal vessels were more hypoxic compared with those surrounding normalized vessels. **D,** Trilocalization of vascular endothelial cells (CD31, red), pericytes (α-SMA, green), and hypoxia (Hpi, cyan) also revealed significantly increased oxygen gradient distance in normalized vessels compared with those lacking pericyte coverage. Images were collected at 100× and 200× magnification. Means ± SEM are shown. Data represent results from $N = 4$ tumors per experimental group and 3 or 4 areas of interest per section. Pimo, pimonidazole. For **A–C**, data were analyzed by one-way analysis of variance with the Tukey multiple comparison test. For **D**, data were analyzed by a paired t test ($N = 20$ sections per experimental group).*, $P < 0.05$; ***, $P < 0.001$; ****, $P < 0.0001$.

viability assay. In our *in vivo* efficacy studies, we never observed signs of NDV(F3aa)-induced toxicity in any mice. Therefore, to investigate the safety of NDV(F3aa) in greater detail, NOSE cells, a minimally transformed human cell line that survives multiple passages, but does not form tumors in mice, were also included in the assay. At each MOI, NOSE cells were the least susceptible to cell death (Fig. 3A). At an MOI of 0.1 only ID8 and CAOV-3 cells showed a drop in viability to 52% and 77% ($P < 0.0001$; Fig. 3B and C), whereas there was no significant change at this MOI in the NOSE cells (Fig. 3A). Additionally, the mean 50% effective concentration (EC_{50}) for each of these cell lines was calculated. CAOV-3 which were most susceptible to NDV(F3aa)-GFP-mediated oncolysis, reached an EC_{50} with an MOI of 0.12, the ID8 cells required almost a 10-fold higher amount of virus at an MOI of 1.1, while NOSE cells did not reach an EC_{50} in this assay. Cytotoxicity was confirmed by microscopy, noted by the presence of cytopathic effect, floating cells and cell counting using trypan blue exclusion at 24, 48, and 72 hours after infection of NDV at an MOI of 0.5. Cell growth curve results showed a 2-fold decrease in cell numbers in ID8 cells ($P < 0.05$) and significant drop in CAOV-3 cells ($P < 0.01$), while no notable changes were seen in NOSE cells (Fig. 3A). Annexin V staining of ID8, CAOV-3, and NOSE cells also confirmed significant cell death by apoptosis in CAOV-3 cells treated with NDV ($P < 0.01$; Supplementary Fig. S2).

Ovarian cells support low levels of NDV(F3aa)-GFP viral protein expression and replication

To evaluate the onset and duration of viral protein expression, ID8 and CAOV-3 cell lines were infected with NDV(F3aa)-GFP at an MOI of 0.5 and expression of the GFP transgene was visualized at various time points p.i. There was restricted expression in ID8 cells at all of the time points as evidenced by the limited number of GFP-positive cells (Fig. 4A). Conversely, infection of CAOV-3 cells with NDV(F3aa)-GFP yielded much higher expression of GFP as early as 8 hours p.i. (Fig. 4B). To investigate the extent to which ID8, CAOV-3, and NOSE cell

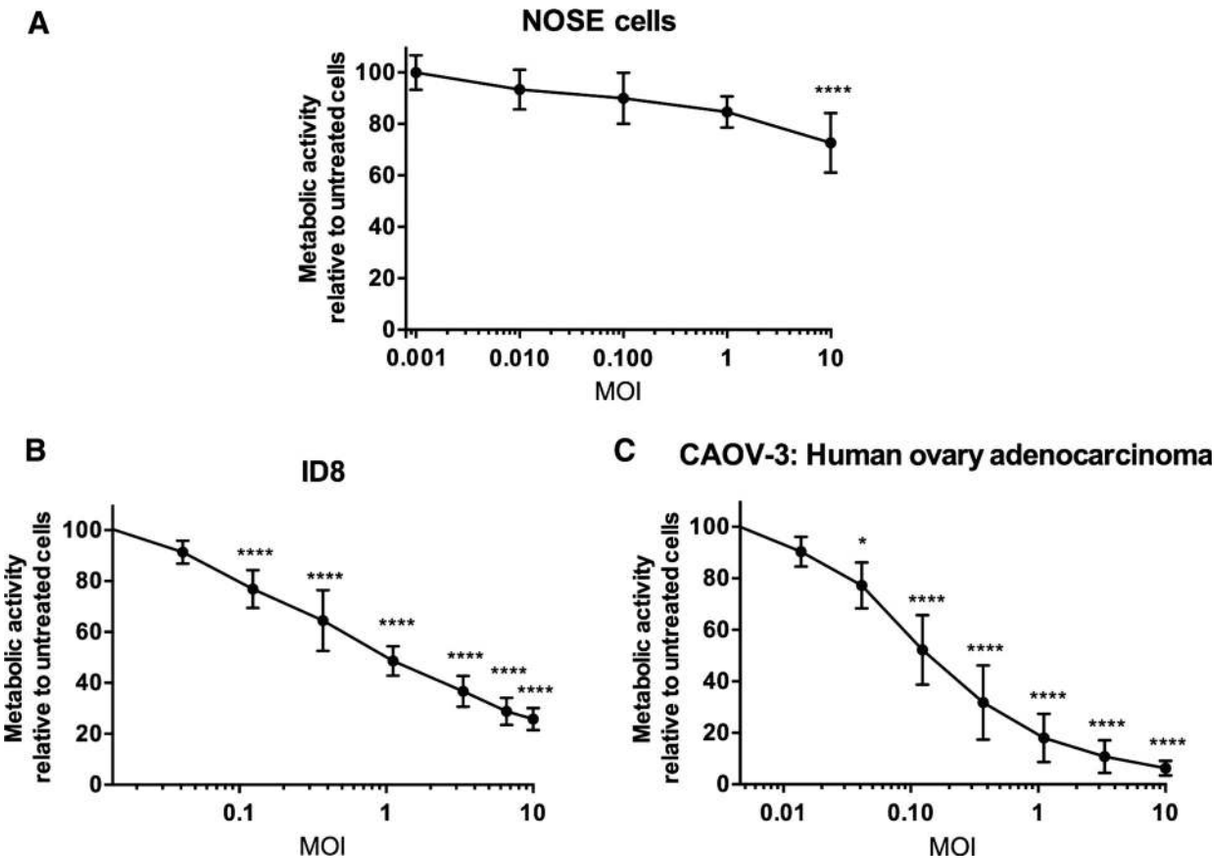

Figure 3.

NDV(F3aa) has direct oncolytic effects on murine and human ovarian cancer cells, but not on NOSE cells. **A,** NOSE cells; **B,** spontaneously transformed murine EOC cells (ID8); and **C**, human EOC cells (CAOV-3) were seeded in triplicate and treated with serial dilutions of NDV(F3aa) for 48 hours. Resazurin was added for an incubation period of 4 hours. The percentage of live cells was determined by normalization to mock-infected controls. Increasing MOI of NDV(F3aa) resulted in decreased metabolic activity of murine and human ovarian cancer cells, but NOSE cells were unaffected at the MOIs tested ($N = 3$). Means ± SEM are shown. Data were analyzed by one-way analysis of variance with the Tukey multiple comparison test (*, $P < 0.05$; ****, $P < 0.0001$) and compares viability at each MOI to untreated cells (MOI of 0).

lines are able to support NDV(F3aa) replication, and viral spread, we generated a single-step viral growth curve. The kinetics of viral replication did not differ between the three cell lines (Fig. 4C).

Lytic and replicative efficacy of NDV(F3aa) in ID8 cells is hindered by sensitivity to interferon

It is well documented that NDV is sensitive to type I IFNs and that defective antiviral signaling is one of the mechanisms that

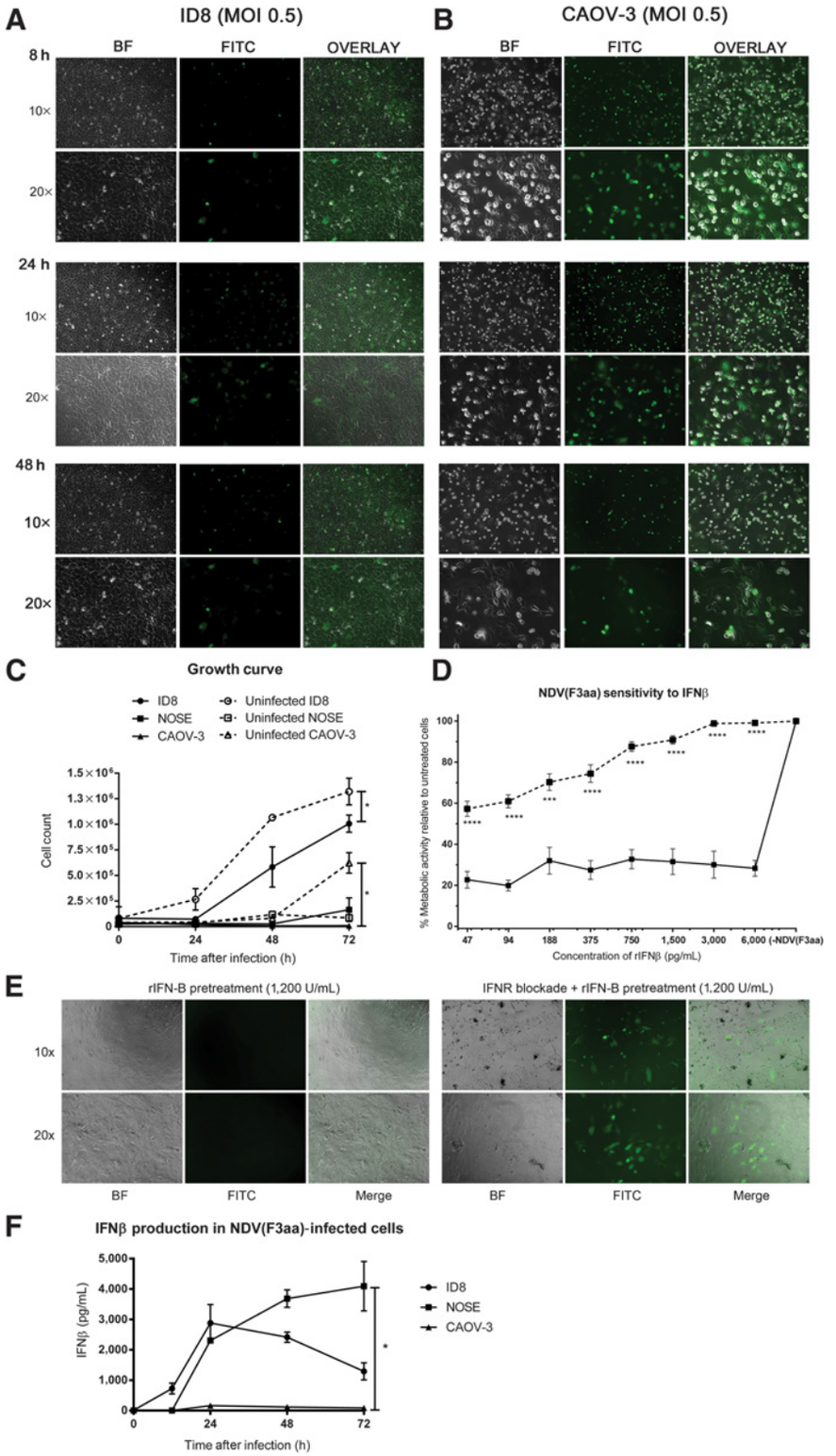

Figure 4.

Murine ID8 cells have limited viral replication but maintain sensitivity to interferon. **A,** Immunofluorescence examination of NDV(F3aa)-GFP-infected ID8 cells (MOI of 0.5) at various time points p.i. revealed limited expression of the GFP transgene in these cells, consistent with low replication. **B,** For direct comparison, CAOV-3 cells were infected with NDV(F3aa)-GFP under the same conditions and revealed a high level of GFP transgene expression. **C,** A one-step viral growth curve was established for NDV(F3aa) in ID8 cells infected at an MOI of 0.5, and supernatant was collected and titered using $TCID_{50}$ after the indicated time points p.i. **D,** Sensitivity of ID8 cells to exogenous type I interferon was demonstrated by pretreating with and without a type I IFN receptor (IFNAR)–blocking antibody for 1 hour, and then IFNβ (0–6,000 pg/mL) was added for 2 hours, followed by NDV(F3aa)-GFP infection at an MOI of 10. **E,** Representative images of NDV(F3aa)-GFP infected cells with (left) only rIFNβ pretreatment or with (right) IFNAR blockade + rIFNβ pretreatment at 48 hours p.i. **F**, ID8 cells were infected at an MOI of 0.01, and supernatant was collected at 4, 12, 24, and 48 hours p.i., in addition to a mock-infected control group. Means ± SEM are shown. Data represent results from three independent experiments ($N = 3$). Data were analyzed using a multiple t test comparing with and without IFNAR blockade results at each time point; ***, $P < 0.001$; ****, $P < 0.0001$. **F,** IFNβ induction in ID8, CAOV-3, and NOSE cells after infection with NDV(F3aa) at an MOI of 0.5. Supernatants were collected at 12, 24, 48, and 72 hours p.i. Levels of IFNβ in the supernatant were assessed by murine and human IFNβ ELISA ($N = 3$). Means ± SEM are shown. Data were analyzed by one-way analysis of variance with the Tukey multiple comparison test; *, $P < 0.05$. h, hours.

contribute to the tumor selective replication of NDV (43–46). To examine whether treatment with IFN would render ID8 cells refractory to NDV(F3aa) infection, these cells were treated with increasing amounts of recombinant mouse IFN (rIFNβ; 0–6,000 pg/mL) 2 hours prior to infection with NDV(F3aa)-GFP at an MOI of 12.5, and cell viability was assessed. To confirm that protection by IFNβ occurs through the IFN receptor, a second experiment was conducted where cells were pretreated with a type I IFN receptor (IFNAR)–blocking antibody for 1 hour prior to treatment with rIFNβ and NDV(F3aa). Assessment of cell viability after 72 hours revealed that ID8 cells are responsive to IFNβ and increased concentrations protected ID8 cells from the cytolytic effects of NDV(F3aa)-GFP (Fig. 4D). Furthermore, this protective effect was ablated in the presence of IFNAR-blocking antibodies. To determine whether pretreatment with rIFNβ also blocks viral protein expression and not just cytotoxic effects of NDV(F3aa)-GFP, we evaluated expression of the GFP transgene at 48 hours p.i. in rIFNβ-treated cells with and without IFNAR blockade. For the rIFNβ-responsive ID8 cell lines, pretreatment with rIFNβ also led to cessation of NDV-mediated transgene expression (Fig. 4E). To assess the extent to which ID8, CAOV-3, and NOSE cells are impaired in their ability to produce IFNβ, cells were infected with NDV (F3aa)-GFP at an MOI of 0.5 and supernatant was collected 12, 24, 48, and 72 hours p.i., and the levels of IFNβ were measured by ELISA. In transformed CAOV-3 and ID8 cells, production of IFNβ peaked at 24 hours p.i. releasing 161 pg/mL and 2,880 pg/mL, respectively (Fig. 4F). Although ID8 cells were able to produce IFNβ in response to NDV(F3aa)-GFP, they did so at a much lower extent than the NOSE cells. CAOV-3 cells produced the lowest amount of IFNβ in response to viral infection. At 72 hours p.i., CAOV-3 cells produced 30× less IFNβ than the NOSE cells ($P < 0.05$).

3TSR-induced vascular normalization enhances trafficking of immunologic cells into primary EOC tumors, especially when combined with NDV(F3aa) treatment

As type I IFNs are potent activators of the immune system, we sought to investigate whether the disease regression seen with 3TSR + NDV(F3aa) treatment correlated with tumor-infiltrating leukocytes. We used IHC analysis against classic immunologic cell markers to investigate the relative intratumoral immune cell trafficking between treatment groups. Compared with controls, treatment with 3TSR alone significantly ($P < 0.05$) enhanced the infiltration of macrophages (Fig. 5A), natural killer (NK) cells (Fig. 5C), and T cells (Fig. 5D and E) into the tumor core. Although NDV(F3aa) treatment alone only improved infiltration of $CD8^+$ leukocytes compared with controls, combining 3TSR + NDV(F3aa) resulted in greater intratumoral influx of macrophages, NK cells, cytotoxic T cells, and T-helper cells compared with either treatment alone (Fig. 5). Combination therapy did not enhance primary tumor infiltration of neutrophils (Fig. 5B) or B cells (Fig. 5F) compared with single treatments.

Effector immune cells induced by 3TSR + NDV(F3aa) treatment are active and proliferating in the tumor core

Given that leukocytes face a number of obstacles to activation within the tumor microenvironment, we wanted to confirm that the increased number of immunologic cells trafficking to the tumor core as a result of 3TSR + NDV(F3aa) were proliferating or expressed markers of activation. We chose to investigate T-cell proliferation and NK cell function, given the significant influx of these lymphocytes into the tumors of our ID8 mouse model following combination treatment (11, 47, 48). Immunofluorescence colocalization on primary tumors revealed a greater proportion of activated NK cells (based on their expression of the early activation marker CD69) in tumors of mice treated with NDV(F3aa; $P < 0.05$), compared with controls or mice treated with 3TSR alone (Fig. 6A). The proportion of activated NK cells was significantly ($P < 0.05$) enhanced in primary tumors of mice treated with 3TSR + NDV (F3aa; Fig. 6A). Likewise, immunofluorescence colocalization of $CD8^+$ T cells and the proliferation marker Ki67 confirmed enhanced influx of proliferating $CD8^+$ T cells in all treatment groups compared with controls (Fig. 6B).

3TSR treatment reduces intratumoral levels of immunosuppressive cytokines

As TSP-1 has been implicated in regulating the tumor microenvironment, we sought to determine whether 3TSR treatment may inhibit the immunosuppressive environment in ovarian tumors. Tumors from control (PBS) mice or mice treated at 60 days PTI were evaluated for the expression of immunosuppressive cytokines VEGF, CCL22, IL6, IL10, and TGFβ1. 3TSR treatment resulted in reduced ($P < 0.05$) levels of all of the immunosuppressive cytokines, compared with PBS controls (Fig. 6C).

Discussion

In the present study, we show a novel opportunity for combination therapy using 3TSR (vascular normalization) and an oncolytic virus to enhance infiltration of leukocytes into primary tumors. In our mouse model of advanced EOC, daily treatment with 3TSR in combination with a one-time intravenous injection of oncolytic NDV(F3aa) resulted in significant disease regression compared with either treatment alone, as evidenced by lower primary tumor size and reduced burden of secondary disease (Fig. 1). As predicted, 3TSR treatment alone did yield some tumor regression in our model, likely as a result of the inhibition of tumor cell proliferation and migration through TGFβ activation via the RFK sequence of 3TSR (49) and direct tumor cell apoptosis via signaling through the CD36 receptor (37). Interestingly, 3TSR treatment on its own increased the number of tumor-infiltrating leukocytes in primary ovarian tumors. Although thrombospondin-1 has been implicated in regulating inflammatory responses (50), its role in tumor immunity has not been studied. This immunogenic effect, combined with its ability to induce tumor cell and tumor endothelial cell apoptosis, may be responsible for its ability to induce regression of advanced-stage ovarian cancer as a single agent (37). NDV(F3aa) injection alone also resulted in tumor regression, which we predicted was likely due to direct oncolysis of tumor cells by the virus. Blanched tumors retrieved from mice treated only with NDV(F3aa) insinuated the phenomenon of vascular shutdown in these tumors. OV-induced vascular shutdown has been established as a consequence of systemic OV therapy with vaccinia virus (a poxvirus) and vesicular stomatitis virus (a rhabdovirus; refs. 22, 51). Our results have extended the phenomenon of vascular shutdown to a third virus, namely, NDV, which is a paramyxovirus. All of these viruses are in human clinical trials and, collectively,

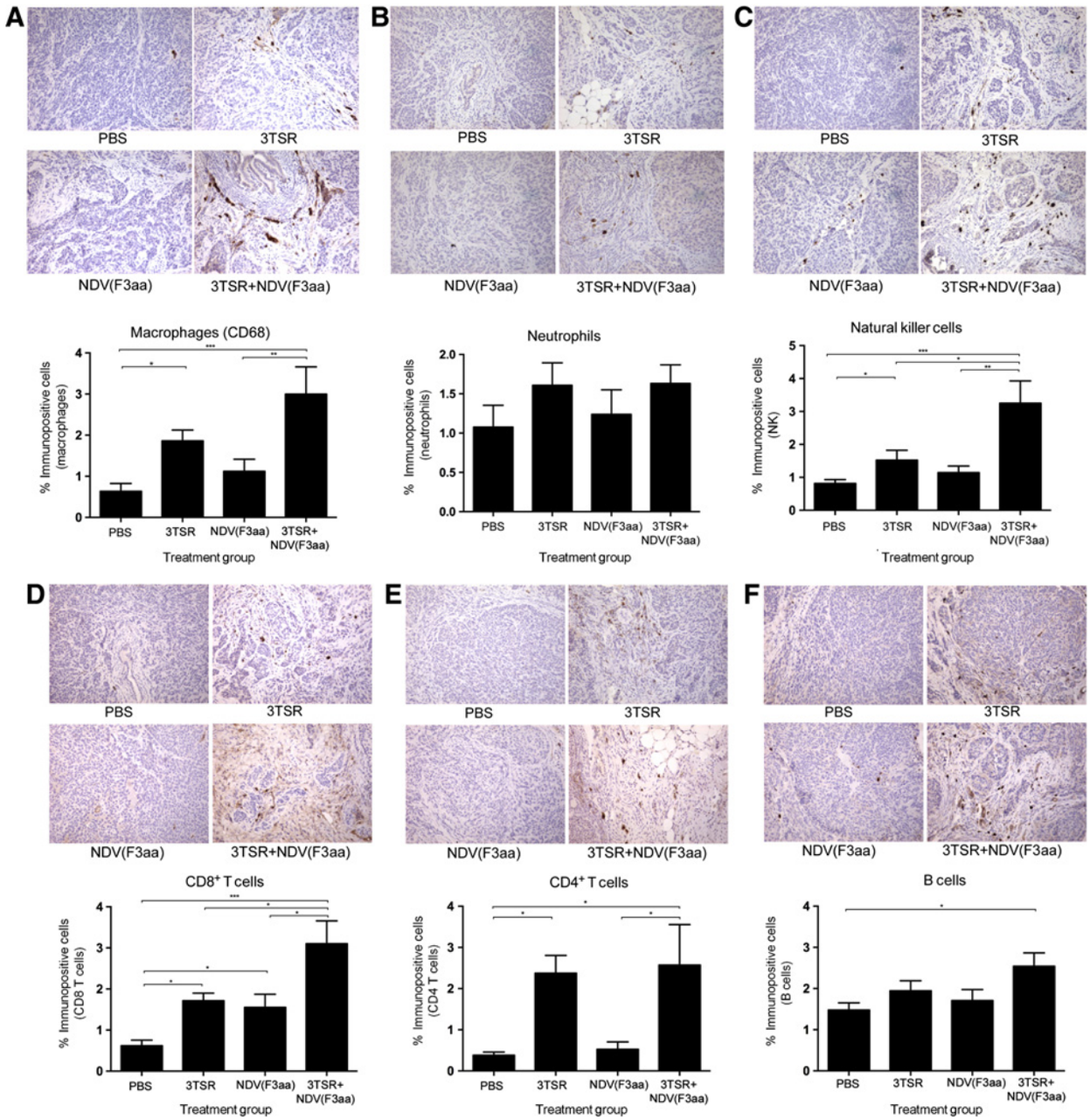

Figure 5.

Combined vascular normalization and oncolytic virus therapy increase immune cell trafficking and tumor uptake. At 90 days PTI, primary tumors were collected from control mice as well as mice treated with 3TSR, NDV(F3aa), or a combination of both. IHC was performed on paraffin-embedded tumor sections by staining for markers against (**A**) macrophages (CD68), (**B**) neutrophils (Ly-6C/G), (**C**) NK cells (NKG2D), (**D**) cytotoxic T cells (CD8), (**E**) T-helper cells (CD4), and (**F**) B/plasma cells (CD138). Treatment with 3TSR enhanced intratumoral infiltration of macrophages, NK cells, cytotoxic T cells, and T-helper cells compared with untreated controls. Although NDV(F3aa) treatment alone did not enhance trafficking of leukocytes, it significantly enhanced intratumoral macrophage, NK cell, and cytotoxic T-cell infiltration in combination with 3TSR. Images were captured at 200× magnification. Means ± SEM are shown. Data represent results from 8 tumors per experimental group and 3 or 4 areas of interest per section. Data were analyzed by one-way analysis of variance with the Tukey multiple comparison test; *, $P < 0.05$; **, $P < 0.01$; ***, $P < 0.001$.

suggest that vascular shutdown may be a relatively common phenomenon among OVs. This OV-induced vascular shutdown is likely to lead to reduced tumor perfusion and increased hypoxia, which are often associated with negative sequelae such as metastases. Further, vascular shutdown would be expected to inhibit recruitment of effector leukocytes into the tumor microenvironment in the hours and days following OV-mediated activation of the immune system.

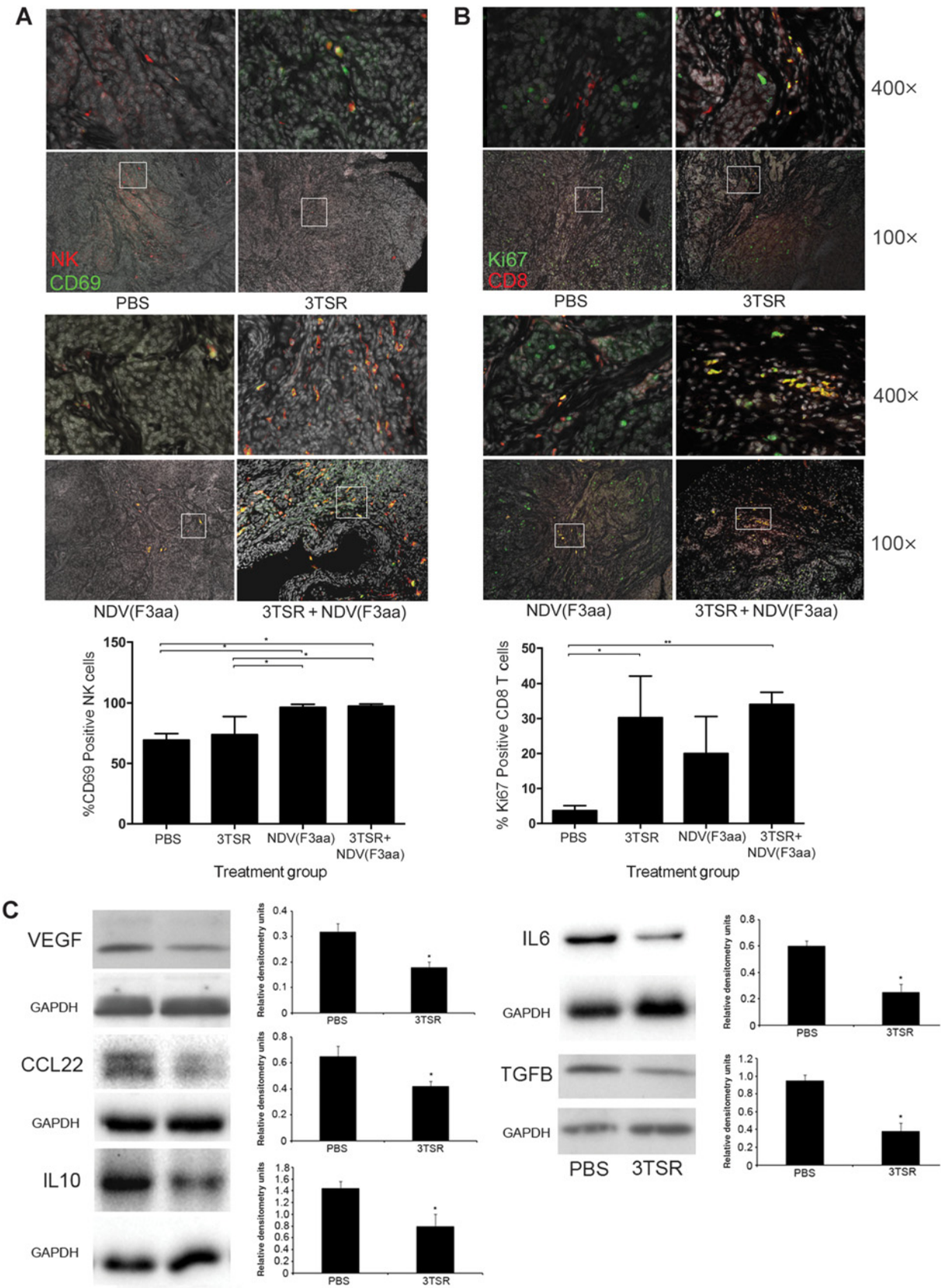

Through analysis of tumor vasculature in treated mice, we determined that treatment with 3TSR induced vascular normalization, as indicated by the presence of luminal, pericyte-covered vessels with significantly enhanced perfusion and reduced tumor hypoxia (Fig. 2). The formation of this normalized vasculature was not hindered by addition of NDV(F3aa) in the combination group. Whereas high VEGF expression in the tumor microenvironment mediates immunosuppression and sensitizes tumor endothelial cells to oncolytic virus infection (21), the reduced VEGF levels brought about by 3TSR intervention may have hindered the ability of NDV(F3aa) to infect tumor vessels and deterred vascular shutdown that results following OV therapy (52). We have shown previously that 3TSR can induce potent tumor vascular normalization and can enhance uptake of chemotherapy drugs (37). In addition to the anti-VEGF effects of 3TSR, vascular pruning and tumor regression was induced by direct binding to its cell-surface receptor CD36, which promotes apoptosis and decreases VEGFR-2 phosphorylation by increasing the expression of SHP-1 (37, 53). As such, 3TSR has multimodal antiangiogenic and antitumor effects and has significant advantage over other antiangiogenic therapies that only target VEGF ligand or receptor. 3TSR is derived from an endogenous glycoprotein and has shown no toxicities. Current work is evaluating the role of Fc-3TSR, a 3TSR fusion protein with a significantly longer half-life in circulation *in vivo*. These characteristics make 3TSR (Fc-3TSR) an attractive compound to be tested clinically.

Treatment with 3TSR also reduced tumor hypoxia significantly, which could improve the efficiency of anticancer agents relying on adequate oxygen levels. Hypoxia has been shown to contribute to immunosuppression in tumors by favoring immune tolerance through enhanced T-regulatory cell differentiation (54, 55). The hypoxic conditions of the tumor microenvironment have also been implicated in inducing tumor cell resistance to cytotoxic T-cell attack (56) and in the suppression of T effector cell function (57). This is relevant considering that in our study, NDV(F3aa) OV monotherapy resulted in reduced vascular supply, as evidenced by blanched tumors, immature vasculature, and increased expression of the hypoxia marker (Fig. 2). By enhancing tumor perfusion ahead of oncolytic virus delivery, 3TSR creates a tumor environment that is optimized for OV efficacy and creates a hospitable environment for immune cells to initiate intratumoral immunity.

In light of the significant tumor inhibition seen *in vivo* with combination 3TSR + NDV(F3aa) therapy, we predicted that the tumoricidal effects of NDV(F3aa) were due, in part, to direct oncolysis. We sought to investigate the oncolytic potential of NDV(F3aa) *in vitro* using spontaneously transformed murine EOC cells (ID8)—the same cell type used in the tumor induction in our mouse model (38). Generally speaking, OVs preferentially replicate in cancerous cells, while sparing normal tissue, due to cancer-specific defects in IFN signaling and other innate antiviral responses (46, 58, 59). Indeed, our own results further demonstrate the ability of an OV to preferentially infect and kill malignant cells, especially in the case of human CAOV-3 cells, which cannot produce IFNβ in response to NDV(F3aa) infection (Figs. 3 and 4). We determined that NDV(F3aa) is a strong inducer of apoptosis in transformed cells, although attempts to titer the virus in tumors were below the limit of detection after 36 hours (not shown).

IFN is critically involved in alerting the cellular immune system to immunogenic mutant cells and thus is one of the most well-established impairments in cancer. Defects in this cytokine pathway include an inability to produce and secret IFN, thereby permitting tumor selective replication of NDV (43–46, 60). In light of work by others showing that infection of transformed cells with NDV(F3aa) is a strong inducer of interferon as a warning signal for imminent threat to surrounding uninfected cells (13, 46), we predicted that the hindered replication of NDV(F3aa) in ID8 cells was likely due to activation of antiviral mechanisms. Indeed, we and others have shown that pretreatment with recombinant IFNβ can abrogate NDV oncolysis and provide complete protection (46, 61–63). This suggests that the susceptibility of ID8 cells in a monoculture to NDV(F3aa)-mediated lysis is likely due to a partial defect in their production of type I IFNs (Fig. 4D and F), although the cells have retained the potential to respond relatively well to IFNs in the extracellular milieu.

It is becoming increasingly clear that the tumor-lysing properties of OVs only partially contribute to the reduction of tumor burden observed in both preclinical and clinical settings (20). In reality, it is the combination of oncolysis and the ability of OVs to initiate systemic antitumor immunity that contributes to the efficacy of this therapeutic modality. Indeed, both *in vitro* and *in vivo* we found there to be limited replication of NDV(F3aa)-GFP (Fig. 4C). These results suggest that the immunostimulatory properties of NDV, rather than direct oncolysis and acute tumor debulking, are likely the dominant mechanism of action contributing to efficacy in this model. When testing the efficacy of NDV(F3aa)-GFP in the ID8 orthotopic syngeneic mouse model of EOC, we did not detect evidence of infectious viruses (the amount of virus present in the tumor was below the limit of detection for this assay) in the tumor at 36 hours p.i. Based on our *in vitro* data, we would anticipate that viral infection led to stimulation of pattern recognition receptors and induction of IFN, which in turn incited an *in situ* antitumor response causing tumor cell death and release of

Figure 6.

Combination therapy results in increased intratumoral immune cell activation and 3TSR reduces expression of immunosuppressive cytokines. At 90 days PTI, primary tumors were collected from control mice as well as mice treated with 3TSR, NDV(F3aa), or a combination of both. Immunofluorescence colocalization was performed by probing tumor sections for both a marker of NK cells (NKG2D; red) and the early activation marker CD69 (green) simultaneously, as well as a marker for cytotoxic T cells (CD8; red) and proliferation (Ki67; green) simultaneously. **A,** NDV(F3aa) and combination treatment [3TSR + NDV(F3aa)] had a higher proportion of activated NK cells compared with PBS controls or 3TSR-treated mice. **B,** Treatment with 3TSR alone or in combination with NDV(F3aa) demonstrated a higher proportion of actively proliferating $CD8^+$ T cells compared with saline controls. Images were captured at 100× and 400× magnification. White boxes in the 100× panels indicate the area selected for 400× magnification. Means ± SEM are shown. Data represent results from 4 tumors per experimental group and 3 or 4 areas of interest per section. Data were analyzed by one-way analysis of variance with Tukey multiple comparison test; *, $P < 0.05$; **, $P < 0.01$. **C,** At 90 days PTI, primary tumors were collected from PBS controls, and mice were treated with 3TSR. Tumor tissue was subjected to Western blot analysis of immunosuppressive cytokines. 3TSR treatment resulted in decreased protein levels of VEGF, CCL22, IL10, IL6, and TGFβ. Densitometric analysis was performed on protein lysates from 3 mice/group, and data are expressed as a ratio of cytokine expression to GAPDH expression. Data were analyzed by one-way analysis of variance with the Tukey multiple comparison test; *, $P < 0.05$.

tumor antigens (64, 65). The type I IFN pathway is emerging as a key player in the induction of antitumor immunity, including innate immune recognition and activation of adaptive immunity, particularly with respect to activation of $CD8^+$ T-cell responses (13, 66, 67), macrophages (68–70), dendritic cells (71), and NK (72) cells. These key responses are likely to have contributed to the reduction in primary tumor size (Fig. 1A), ascites fluid production (Supplementary Fig. S1), and secondary lesion formation (Fig. 1B) observed in this study.

We viewed this sensitivity of NDV(F3aa) to interferon as a benefit for the viral platform, given that this sensitivity is likely the reason NDV is limited to causing pathogenesis in avian species (73). In confirmation of the high safety profile of NDV(F3aa), we showed that NOSE cells, which are able to produce IFNβ (Fig. 4F), are refractory to viral oncolysis at lower, clinically relevant doses of NDV *in vitro* (Fig. 3A). The fact that NDV failed to replicate well in ID8 and CAOV-3 cells is interesting in the context of the remarkable efficacy that could be achieved with this virus in conjunction with vascular normalization. We showed that cell death and viral protein expression was much better in human CAOV-3 cells (Figs. 3C and 4A), and this was likely due to the significant impairment in IFNβ production (Fig. 4F) and predict that the efficacy of our novel therapeutic strategy would be potentiated in tumors that better support direct viral oncolysis and immune activation. In fact, significant therapeutic efficacy of NDV(F3aa) *in vivo*, despite mediocre NDV(F3aa)-mediated cell lysis *in vitro*, suggested to us that the effects of 3TSR and NDV(F3aa) on disease regression in advanced-stage EOC might be immune-mediated, rather than predominantly oncolytic. In accordance with this idea, we observed enhanced infiltration of macrophages, NK cells, and T-helper cells in the tumor cores of mice treated with 3TSR only, and also enhanced cytotoxic T-cell and B-cell infiltration when 3TSR was combined with NDV (F3aa; Fig. 5). The ability of 3TSR to increase infiltration of leukocytes could be due to the enhanced perfusion with bloodborne cells as a direct result of vascular normalization (74). In addition, VEGF is a potent inhibitor of adhesion molecules such as ICAM-1 and VCAM-1 on the surface of endothelial cells, and leukocytes tend to utilize these molecules for extravasation into the tumor (75). Therefore, the significantly improved influx of leukocytes into 3TSR-treated tumors may not only reflect greater perfusion but also enhanced diapedesis through tumor vasculature.

The combination of 3TSR and NDV(F3aa) therapy also increased the activation of NK cells within primary tumors. This heightened activation may have been due to a direct response to the virally infected cells, given that the proportion of activated NK cells was lessened in tumors of mice treated with 3TSR or PBS alone. Treatment with NDV(F3aa) also enhanced the proliferation of $CD8^+$ T cells recruited to primary tumors. Interestingly, proliferation of cytotoxic T cells was also enhanced with 3TSR treatment alone, which appears to be a novel consequence of treatment with the TSP-1 type I repeat region. One mechanism by which 3TSR may facilitate recruitment and uptake of cytotoxic leukocytes is by reducing the intratumoral immunosuppressive environment. Many tumors, including ovarian, are known to upregulate the expression of immunosuppressive cytokines in order to inhibit immune cell recruitment and destruction of tumor cells (76). 3TSR treatment resulted in decreased expression of potent immunosuppressive cytokines such as VEGF, CCL22, IL10, IL6, and TGFβ (Fig. 6C). TSP-1 has been shown to have a direct anti-inflammatory effect, inhibiting expression of cytokines such as VEGF and IL6. Also, vascular normalization and decreased tumor hypoxia inhibits immunosuppression within the tumor microenvironment and results in tumor immunostimulation (77). By reducing the immunosuppressive environment, 3TSR treatment may act to facilitate immune cell recruitment by NDV(F3aa) and enhanced tumor uptake of these cells via vascular normalization. Given the high propensity of chemoresistance in advanced-stage ovarian cancer, combined 3TSR and NDV (F3aa) therapy may have important clinical implications by increasing immunogenic cell death and inhibiting the immunosuppressive tumor environment to resensitize chemoresistant ovarian cancer cells (78). Our ability to enhance uptake and activation of leukocytes and increase the $CD8^+$/regulatory T-cell ratio could reduce the chemoresistance seen in advanced-stage ovarian cancer.

The data presented here further establish the ability of 3TSR to induce vascular normalization and facilitate delivery of anticancer agents to solid tumors. We have used an immunocompetent murine mouse model of EOC that has similarities to human ovarian cancer and relevance to guide clinical development of human therapies. In this study, we have shown that 3TSR improves the trafficking of leukocytes into EOC primary tumors and causes significant disease regression of advanced-stage EOC when combined with an oncolytic virus. We have also extended previous findings that NDV(F3aa) is a useful immunotherapeutic agent, given its broad safety margin and potent immunostimulatory effects. Clinical benefit has been observed by several investigators, and our studies have shown efficacy in advanced metastatic disease, including patients with chemotherapy-resistant ovarian carcinoma (17). The combined ability of 3TSR and NDV(F3aa) to target multiple aspects of the tumor microenvironment makes this therapeutic approach attractive for the treatment of advanced-stage ovarian cancer, which typically overcomes single-agent therapy and becomes chemoresistant. There are no current effective strategies for overcoming chemoresistant disease, and novel combination therapies are needed. This study provides proof of principle that vascular normalization can potentiate OV-based immunotherapy for the treatment of both primary and metastatic EOC. Further, it challenges the common hypothesis in the field of oncolytic virotherapy that vascular shutdown is a requisite or desired consequence for effective treatment of cancers. Importantly, this therapeutic approach has excellent translational potential because it is based on an oncolytic virus platform that has an extremely long history of testing in human patients (79) combined with a polypeptide that is highly amenable to cost-effective manufacturing under Good Manufacturing Practice conditions.

Disclosure of Potential Conflicts of Interest

No potential conflicts of interest were disclosed.

Authors' Contributions

Conception and design: K. Matuszewska, L.A. Santry, J. Lawler, S.K. Wootton, B.W. Bridle, J. Petrik

Development of methodology: K. Matuszewska, L.A. Santry, S.K. Wootton, B.W. Bridle, J. Petrik

Acquisition of data (provided animals, acquired and managed patients, provided facilities, etc.): K. Matuszewska, L.A. Santry, J.P. van Vloten, A.W.K. Au Yeung, S.K. Wootton, B.W. Bridle, J. Petrik

Analysis and interpretation of data (e.g., statistical analysis, biostatistics, computational analysis): K. Matuszewska, L.A. Santry, J.P. van Vloten, J. Lawler, S.K. Wootton, B.W. Bridle, J. Petrik
Writing, review, and/or revision of the manuscript: K. Matuszewska, L.A. Santry, P.P. Major, J. Lawler, S.K. Wootton, B.W. Bridle, J. Petrik
Administrative, technical, or material support (i.e., reporting or organizing data, constructing databases): K. Matuszewska, L.A. Santry, P.P. Major, J. Petrik
Study supervision: S.K. Wootton, B.W. Bridle, J. Petrik

Acknowledgments

The authors would like to acknowledge technical support from Kata Osz, Sara Marcine, and Mark Duquette on this project. This work was supported by material contribution from P. Major and operating grants to J. Petrik from the Canadian Institutes for Health Research, Cancer Research Society, and Ovarian Cancer Canada. The Bridle lab was funded by the Terry Fox Research Institute (New Investigator Award, project #1041). The Wootton lab was funded by the Canadian Institutes for Health Research and NSERC Engage. The project was also supported by a CAO Pilot Grant from the Beth Israel Deaconess Medical Center.

The costs of publication of this article were defrayed in part by the payment of page charges. This article must therefore be hereby marked *advertisement* in accordance with 18 U.S.C. Section 1734 solely to indicate this fact.

Received January 19, 2018; revised May 3, 2018; accepted September 7, 2018; published first September 11, 2018.

References

1. Siegel RL, Miller KD, Jemal A. Cancer statistics, 2018. CA Cancer J Clin 2018;68:7–30.
2. Gajjar K, Ogden G, Mujahid MI, Razvi K. Symptoms and risk factors of ovarian cancer: a survey in primary care. ISRN Obstet Gynecol 2012; 2012:754197.
3. Cristea M, Han E, Salmon L, Morgan RJ. Practical considerations in ovarian cancer chemotherapy. Ther Adv Med Oncol 2010;2:175–87.
4. Bast RC Jr, Hennessy B, Mills GB. The biology of ovarian cancer: new opportunities for translation. Nat Rev Cancer 2009;9:415–28.
5. Dunn GP, Bruce AT, Ikeda H, Old LJ, Schreiber RD. Cancer immunoediting: from immunosurveillance to tumor escape. Nat Immunol 2002;3:991–8.
6. Shankaran V, Ikeda H, Bruce AT, White JM, Swanson PE, Old LJ, et al. IFNgamma and lymphocytes prevent primary tumour development and shape tumour immunogenicity. Nature 2001;410:1107–11.
7. Smyth MJ. Multiple approaches to immunotherapy – the new pillar of cancer treatment. Immunol Cell Biol 2017;95:323–4.
8. Anassi E, Ndefo UA. Sipuleucel-T (provenge) injection: the first immunotherapy agent (vaccine) for hormone-refractory prostate cancer. P T 2011;36:197–202.
9. Kwok G, Yau TC, Chiu JW, Tse E, Kwong YL. Pembrolizumab (Keytruda). Hum Vaccin Immunother 2016;12:2777–89.
10. Kloudova K, Hromadkova H, Partlova S, Brtnicky T, Rob L, Bartunkova J, et al. Expression of tumor antigens on primary ovarian cancer cells compared to established ovarian cancer cell lines. Oncotarget 2016;7: 46120–6.
11. Zhang L, Conejo-Garcia JR, Katsaros D, Gimotty PA, Massobrio M, Regnani G, et al. Intratumoral T cells, recurrence, and survival in epithelial ovarian cancer. N Engl J Med 2003;348:203–13.
12. Kaufman HL, Kohlhapp FJ, Zloza A. Oncolytic viruses: a new class of immunotherapy drugs. Nat Rev Drug Discov 2015;14:642–62.
13. Zamarin D, Holmgaard RB, Subudhi SK, Park JS, Mansour M, Palese P, et al. Localized oncolytic virotherapy overcomes systemic tumor resistance to immune checkpoint blockade immunotherapy. Sci Transl Med 2014;6: 226ra32.
14. Zamarin D, Palese P. Oncolytic Newcastle disease virus for cancer therapy: old challenges and new directions. Future Microbiol 2012;7:347–67.
15. Liang W, Wang H, Sun TM, Yao WQ, Chen LL, Jin Y, et al. Application of autologous tumor cell vaccine and NDV vaccine in treatment of tumors of digestive tract. World J Gastroenterol 2003;9:495–8.
16. Ahlert T, Sauerbrei W, Bastert G, Ruhland S, Bartik B, Simiantonaki N, et al. Tumor-cell number and viability as quality and efficacy parameters of autologous virus-modified cancer vaccines in patients with breast or ovarian cancer. J Clin Oncol 1997;15:1354–66.
17. Hotte SJ, Lorence RM, Hirte HW, Polawski SR, Bamat MK, O'Neil JD, et al. An optimized clinical regimen for the oncolytic virus PV701. Clin Cancer Res 2007;13:977–85.
18. Pomer S, Schirrmacher V, Thiele R, Lohrke H, Brkovic D, Staehler G. Tumor response and 4 year survival-data of patients with advanced renal-cell carcinoma treated with autologous tumor vaccine and subcutaneous R-IL-2 and IFN-alpha(2b). Int J Oncol 1995;6:947–54.
19. Panda A, Huang Z, Elankumaran S, Rockemann DD, Samal SK. Role of fusion protein cleavage site in the virulence of Newcastle disease virus. Microb Pathog 2004;36:1–10.
20. Lichty BD, Breitbach CJ, Stojdl DF, Bell JC. Going viral with cancer immunotherapy. Nat Rev Cancer 2014;14:559–67.
21. Arulanandam R, Batenchuk C, Angarita FA, Ottolino-Perry K, Cousineau S, Mottashed A, et al. VEGF-mediated induction of PRD1-BF1/Blimp1 expression sensitizes tumor vasculature to oncolytic virus infection. Cancer Cell 2015;28:210–24.
22. Breitbach CJ, De Silva NS, Falls TJ, Aladl U, Evgin L, Paterson J, et al. Targeting tumor vasculature with an oncolytic virus. Mol Ther 2011; 19:886–94.
23. Breitbach CJ, Arulanandam R, De Silva N, Thorne SH, Patt R, Daneshmand M, et al. Oncolytic vaccinia virus disrupts tumor-associated vasculature in humans. Cancer Res 2013;73:1265–75.
24. Kottke T, Hall G, Pulido J, Diaz RM, Thompson J, Chong H, et al. Antiangiogenic cancer therapy combined with oncolytic virotherapy leads to regression of established tumors in mice. J Clin Invest 2010;120:1551–60.
25. Woller N, Gurlevik E, Ureche CI, Schumacher A, Kuhnel F. Oncolytic viruses as anticancer vaccines. Front Oncol 2014;4:188.
26. Weis SM, Cheresh DA. Tumor angiogenesis: molecular pathways and therapeutic targets. Nat Med 2011;17:1359–70.
27. Morikawa S, Baluk P, Kaidoh T, Haskell A, Jain RK, McDonald DM. Abnormalities in pericytes on blood vessels and endothelial sprouts in tumors. Am J Pathol 2002;160:985–1000.
28. Jain RK. Delivery of novel therapeutic agents in tumors: physiological barriers and strategies. J Natl Cancer Inst 1989;81:570–6.
29. Huang L, Ao Q, Zhang Q, Yang X, Xing H, Li F, et al. Hypoxia induced paclitaxel resistance in human ovarian cancers via hypoxia-inducible factor 1alpha. J Cancer Res Clin Oncol 2010;136:447–56.
30. Carmeliet P, Jain RK. Principles and mechanisms of vessel normalization for cancer and other angiogenic diseases. Nat Rev Drug Discov 2011; 10:417–27.
31. Yuan F, Chen Y, Dellian M, Safabakhsh N, Ferrara N, Jain RK. Time-dependent vascular regression and permeability changes in established human tumor xenografts induced by an anti-vascular endothelial growth factor/vascular permeability factor antibody. Proc Natl Acad Sci U S A 1996;93:14765–70.
32. Meadows KL, Hurwitz HI. Anti-VEGF therapies in the clinic. Cold Spring Harb Perspect Med 2012;2. pii: a006577.
33. Good DJ, Polverini PJ, Rastinejad F, Le Beau MM, Lemons RS, Frazier WA, et al. A tumor suppressor-dependent inhibitor of angiogenesis is immunologically and functionally indistinguishable from a fragment of thrombospondin. Proc Natl Acad Sci U S A 1990;87:6624–8.
34. Greenaway J, Lawler J, Moorehead R, Bornstein P, Lamarre J, Petrik J. Thrombospondin-1 inhibits VEGF levels in the ovary directly by binding and internalization via the low density lipoprotein receptor-related protein-1 (LRP-1). J Cell Physiol 2007;210:807–18.
35. Zhang X, Galardi E, Duquette M, Delic M, Lawler J, Parangi S. Antiangiogenic treatment with the three thrombospondin-1 type 1 repeats recombinant protein in an orthotopic human pancreatic cancer model. Clin Cancer Res 2005;11:2337–44.
36. Tolsma SS, Volpert OV, Good DJ, Frazier WA, Polverini PJ, Bouck N. Peptides derived from two separate domains of the matrix protein thrombospondin-1 have anti-angiogenic activity. J Cell Biol 1993; 122:497–511.
37. Russell S, Duquette M, Liu J, Drapkin R, Lawler J, Petrik J. Combined therapy with thrombospondin-1 type I repeats (3TSR) and chemotherapy induces regression and significantly improves survival in a preclinical

model of advanced stage epithelial ovarian cancer. FASEB J 2015;29: 576–88.
38. Greenaway J, Henkin J, Lawler J, Moorehead R, Petrik J. ABT-510 induces tumor cell apoptosis and inhibits ovarian tumor growth in an orthotopic, syngeneic model of epithelial ovarian cancer. Mol Cancer Ther 2009;8:64–74.
39. Santry LA, McAusland TM, Susta L, Wood GA, Major PP, Petrik JJ, et al. Production and purification of high-titer Newcastle disease virus for use in preclinical mouse models of cancer. Mol Ther Methods Clin Dev 2018;9:181–91.
40. Ramakrishnan MA. Determination of 50% endpoint titer using a simple formula. World J Virol 2016;5:85–6.
41. Arteel GE, Thurman RG, Raleigh JA. Reductive metabolism of the hypoxia marker pimonidazole is regulated by oxygen tension independent of the pyridine nucleotide redox state. Eur J Biochem 1998; 253:743–50.
42. Varia MA, Calkins-Adams DP, Rinker LH, Kennedy AS, Novotny DB, Fowler WC Jr, et al. Pimonidazole: a novel hypoxia marker for complementary study of tumor hypoxia and cell proliferation in cervical carcinoma. Gynecol Oncol 1998;71:270–7.
43. Fiola C, Peeters B, Fournier P, Arnold A, Bucur M, Schirrmacher V. Tumor selective replication of Newcastle disease virus: association with defects of tumor cells in antiviral defence. Int J Cancer 2006;119:328–38.
44. Wilden H, Fournier P, Zawatzky R, Schirrmacher V. Expression of RIG-I, IRF3, IFN-beta and IRF7 determines resistance or susceptibility of cells to infection by Newcastle disease virus. Int J Oncol 2009;34:971–82.
45. Critchley-Thorne RJ, Simons DL, Yan N, Miyahira AK, Dirbas FM, Johnson DL, et al. Impaired interferon signaling is a common immune defect in human cancer. Proc Natl Acad Sci U S A 2009;106:9010–5.
46. Krishnamurthy S, Takimoto T, Scroggs RA, Portner A. Differentially regulated interferon response determines the outcome of Newcastle disease virus infection in normal and tumor cell lines. J Virol 2006; 80:5145–55.
47. Carlsten M, Bjorkstrom NK, Norell H, Bryceson Y, van Hall T, Baumann BC, et al. DNAX accessory molecule-1 mediated recognition of freshly isolated ovarian carcinoma by resting natural killer cells. Cancer Res 2007;67:1317–25.
48. Sato E, Olson SH, Ahn J, Bundy B, Nishikawa H, Qian F, et al. Intraepithelial CD8+ tumor-infiltrating lymphocytes and a high CD8+/regulatory T cell ratio are associated with favorable prognosis in ovarian cancer. Proc Natl Acad Sci U S A 2005;102:18538–43.
49. Miao WM, Seng WL, Duquette M, Lawler P, Laus C, Lawler J. Thrombospondin-1 type 1 repeat recombinant proteins inhibit tumor growth through transforming growth factor-beta-dependent and -independent mechanisms. Cancer Res 2001;61:7830–9.
50. Lopez-Dee Z, Pidcock K, Gutierrez LS. Thrombospondin-1: multiple paths to inflammation. Mediators Inflamm 2011;2011:296069.
51. Mahoney DJ, Stojdl DF. Molecular pathways: multimodal cancer-killing mechanisms employed by oncolytic vesiculoviruses. Clin Cancer Res 2013;19:758–63.
52. Liu TC, Hwang T, Park BH, Bell J, Kirn DH. The targeted oncolytic poxvirus JX-594 demonstrates antitumoral, antivascular, and anti-HBV activities in patients with hepatocellular carcinoma. Mol Ther 2008;16:1637–42.
53. Chu LY, Ramakrishnan DP, Silverstein RL. Thrombospondin-1 modulates VEGF signaling via CD36 by recruiting SHP-1 to VEGFR2 complex in microvascular endothelial cells. Blood 2013;122:1822–32.
54. Curiel TJ, Coukos G, Zou L, Alvarez X, Cheng P, Mottram P, et al. Specific recruitment of regulatory T cells in ovarian carcinoma fosters immune privilege and predicts reduced survival. Nat Med 2004;10:942–9.
55. Westendorf AM, Skibbe K, Adamczyk A, Buer J, Geffers R, Hansen W, et al. Hypoxia enhances immunosuppression by inhibiting CD4+ effector T cell function and promoting treg activity. Cell Physiol Biochem 2017;41:1271–84.
56. Noman MZ, Buart S, Van Pelt J, Richon C, Hasmim M, Leleu N, et al. The cooperative induction of hypoxia-inducible factor-1 alpha and STAT3 during hypoxia induced an impairment of tumor susceptibility to CTL-mediated cell lysis. J Immunol 2009;182:3510–21.
57. Palazon A, Aragones J, Morales-Kastresana A, de Landazuri MO, Melero I. Molecular pathways: hypoxia response in immune cells fighting or promoting cancer. Clin Cancer Res 2012;18:1207–13.
58. Stojdl DF, Lichty B, Knowles S, Marius R, Atkins H, Sonenberg N, et al. Exploiting tumor-specific defects in the interferon pathway with a previously unknown oncolytic virus. Nat Med 2000;6:821–5.
59. Vigil A, Park MS, Martinez O, Chua MA, Xiao S, Cros JF, et al. Use of reverse genetics to enhance the oncolytic properties of Newcastle disease virus. Cancer Res 2007;67:8285–92.
60. Fournier P, Wilden H, Schirrmacher V. Importance of retinoic acid-inducible gene I and of receptor for type I interferon for cellular resistance to infection by Newcastle disease virus. Int J Oncol 2012;40:287–98.
61. Park MS, Shaw ML, Munoz-Jordan J, Cros JF, Nakaya T, Bouvier N, et al. Newcastle disease virus (NDV)-based assay demonstrates interferon-antagonist activity for the NDV V protein and the Nipah virus V, W, and C proteins. J Virol 2003;77:1501–11.
62. Puhlmann J, Puehler F, Mumberg D, Boukamp P, Beier R. Rac1 is required for oncolytic NDV replication in human cancer cells and establishes a link between tumorigenesis and sensitivity to oncolytic virus. Oncogene 2010;29:2205–16.
63. Ruotsalainen JJ, Kaikkonen MU, Niittykoski M, Martikainen MW, Lemay CG, Cox J, et al. Clonal variation in interferon response determines the outcome of oncolytic virotherapy in mouse CT26 colon carcinoma model. Gene Ther 2015;22:65–75.
64. Meurs E, Chong K, Galabru J, Thomas NS, Kerr IM, Williams BR, et al. Molecular cloning and characterization of the human double-stranded RNA-activated protein kinase induced by interferon. Cell 1990;62:379–90.
65. Thompson MR, Kaminski JJ, Kurt-Jones EA, Fitzgerald KA. Pattern recognition receptors and the innate immune response to viral infection. Viruses 2011;3:920–40.
66. Diamond MS, Kinder M, Matsushita H, Mashayekhi M, Dunn GP, Archambault JM, et al. Type I interferon is selectively required by dendritic cells for immune rejection of tumors. J Exp Med 2011;208:1989–2003.
67. Fuertes MB, Kacha AK, Kline J, Woo SR, Kranz DM, Murphy KM, et al. Host type I IFN signals are required for antitumor CD8+ T cell responses through CD8{alpha}+ dendritic cells. J Exp Med 2011;208:2005–16.
68. Hrabak A, Csuka I, Bajor T, Csatary LK. The cytotoxic anti-tumor effect of MTH-68/H, a live attenuated Newcastle disease virus is mediated by the induction of nitric oxide synthesis in rat peritoneal macrophages in vitro. Cancer Lett 2006;231:279–89.
69. Schirrmacher V, Bai L, Umansky V, Yu L, Xing Y, Qian Z. Newcastle disease virus activates macrophages for anti-tumor activity. Int J Oncol 2000; 16:363–73.
70. Umansky V, Shatrov VA, Lehmann V, Schirrmacher V. Induction of NO synthesis in macrophages by Newcastle disease virus is associated with activation of nuclear factor-kappa B. Int Immunol 1996;8: 491–8.
71. Bai L, Koopmann J, Fiola C, Fournier P, Schirrmacher V. Dendritic cells pulsed with viral oncolysates potently stimulate autologous T cells from cancer patients. Int J Oncol 2002;21:685–94.
72. Jarahian M, Watzl C, Fournier P, Arnold A, Djandji D, Zahedi S, et al. Activation of natural killer cells by Newcastle disease virus hemagglutinin-neuraminidase. J Virol 2009;83:8108–21.
73. Park MS, Garcia-Sastre A, Cros JF, Basler CF, Palese P. Newcastle disease virus V protein is a determinant of host range restriction. J Virol 2003;77:9522–32.
74. Huang Y, Yuan J, Righi E, Kamoun WS, Ancukiewicz M, Nezivar J, et al. Vascular normalizing doses of antiangiogenic treatment reprogram the immunosuppressive tumor microenvironment and enhance immunotherapy. Proc Natl Acad Sci U S A 2012;109:17561–6.
75. Motz GT, Coukos G. Deciphering and reversing tumor immune suppression. Immunity 2013;39:61–73.
76. Yigit R, Massuger LF, Zusterzeel PL, Pots J, Figdor CG, Torensma R. Cytokine profiles in cyst fluids from ovarian tumors reflect immunosuppressive state of the tumor. Int J Gynecol Cancer 2011;21:1241–7.
77. Mpekris F, Baish JW, Stylianopoulos T, Jain RK. Role of vascular normalization in benefit from metronomic chemotherapy. Proc Natl Acad Sci U S A 2017;114:1994–9.
78. Wang W, Kryczek I, Dostal L, Lin H, Tan L, Zhao L, et al. Effector T cells abrogate stroma-mediated chemoresistance in ovarian cancer. Cell 2016;165:1092–105.
79. Cassel WA, Garrett RE. Newcastle disease virus as an antineoplastic agent. Cancer 1965;18:863–8.